Electronic Journal of Differential Equations, Vol. 2020 (2020), No. 64, pp. 1–17.
ISSN: 1072-6691. URL: http://ejde.math.txstate.edu or http://ejde.math.unt.edu

ASSESSING THE EFFICIENCY OF DIFFERENT CONTROL STRATEGIES FOR THE COVID-19 EPIDEMIC

CÉSAR CASTILHO, JOÃO A. M. GONDIM,
MARCELO MARCHESIN, MEHRAN SABETI

Abstract. The goal of this work is to analyze the effects of control policies for the coronavirus (COVID-19) epidemic in Brazil. This is done by considering an age-structured SEIR model with a quarantine class and two types of controls. The first one studies the sensitivity with regard to the parameters of the basic reproductive number R_0 which is calculated by a next generation method. The second one evaluates different quarantine strategies by comparing their relative total number of deaths.

1. Introduction

At the end of 2019 several cases of pneumonia of unknown etiology were detected in Wuhan City in the Chinese province of Hubei. The Chinese Country Office of the World Health Organization (Website https://www.who.int) was informed and reported that a novel coronavirus (officially named COVID-19) was identified on January 7, 2020, as the cause of such infection. The imminent potential for worldwide spread was soon recognized and an international alert was issued.

COVID-19 was shown to be very lethal and easily spreading. Before the end of January [19, 13] as many as $75,000$ infected cases were estimated in Wuhan City. On March 11, because of the seriousness of the situation, the WHO declared it a Pandemic.

The goal of this study is to assess through the analysis of a differential equations model the importance of different control policies for the Brazilian COVID-19 epidemic. Even though Brazil is considered for the scope of this paper, the techniques and tools used in this study can be easily adapted for any other country. The impact of different control strategies are qualitatively evaluated and mathematically based guidelines concerning different protective measures and quarantine strategies are formulated. The article is organized as follows: In Section 2, the age-structured SEIR model with quarantine is formulated. Demographic data from Brazil is introduced and discussed. In Section 3, the classical SEIR model without vital dynamics and with a quarantine compartment is studied. The goals here are, firstly, to adjust parameters and to fit the real data, and secondly, to study the necessary quarantine efforts and times so to be able to influence the epidemic. In Section 4, the parameters for the age-structured model are adjusted (using the

2010 *Mathematics Subject Classification.* 92D30, 93C15, 34H05.
Key words and phrases. Coronavirus; quarantine; epidemic; SEIR models.

Submitted April 6, 2020. Published June 24, 2020.

ones calculated on the previous section). The next generation approach is used to calculate the basic reproduction number and a deterministic sensibility analysis of R_0 [5] is carried on. In Section 5, different quarantine strategies for different age classes are considered and compared. We draw our conclusions in Section 6.

2. Age-structured SEIR model

The outbreak of COVID-19 has shown a markedly low proportion of children among reported cases [17, 16]. More generally, it has been observed that the number of cases and the risk of severe disease rise as age increases [4, 15, 20]. Understanding the role of age in transmission and disease severity is critical for determining the likely impact of control measures for decreasing transmission [6]. A classical SEIR model is used with the addition of a quarantine class as proposed in [11]. Since age is such an important factor on the COVID-19 epidemic, it will be assumed that the population is age-structured (see [2, 9, 18] for continuous models and [21, 22] for discrete models). Three age classes are used; infants with ages in the interval $[0, 19]$ ($i = 1$), adults with ages in the interval $[20, 59]$ ($i = 2$), and elderly with ages in the interval $[60, 100]$ ($i = 3$). The proportion of each age class in the Brazilian population is shown in Table 1 (see [10]).

Let $S_i(t)$, $E_i(t)$, $I_i(t)$, $R_i(t)$ and $Q_i(t)$ represent the number of susceptibles, exposed, infected, removed and quarantined at age class i respectively at time $t \geq 0$. The equations are as follows

$$\begin{aligned}
Q_i'(t) &= p_i S_i(t) - \lambda_i Q_i(t), \quad i = 1, 2, 3, \\
S_1'(t) &= \Lambda - (\mu_1 + \rho_1) S_1(t) - S_1(t)\Big(\sum_{j=1}^{3} \beta_{1j} I_j(t)\Big) \\
&\quad - p_1 S_1(t) + \lambda_1 Q_1(t)\,, \\
S_2'(t) &= \rho_1 S_1(t) - (\mu_2 + \rho_2) S_2(t) - S_2(t)\Big(\sum_{j=1}^{3} \beta_{2j} I_j(t)\Big) \\
&\quad - p_2 S_2(t) + \lambda_2 Q_2(t)\,, \\
S_3'(t) &= \rho_2 S_2(t) - \mu_3 S_3(t) - S_3(t)\Big(\sum_{j=1}^{3} \beta_{3j} I_j(t)\Big) \\
&\quad - p_3 S_3(t) + \lambda_3 Q_3(t)\,, \\
E_i'(t) &= S_i(t)\Big(\sum_{j=i}^{3} \beta i j I_j(t)\Big) - (\sigma_i + \mu_i)\, E_i(t)\,, \\
I_i'(t) &= \sigma_i\, E_i(t) - (\gamma_i + \mu_i + m_i) I_i(t)\,, \\
R_i'(t) &= \gamma I_i(t) - \mu_i\, R_i(t)\,,
\end{aligned} \tag{2.1}$$

The parameters are all non-negative (or positive) and are described in Table 2. p_i and λ_i are the quarantine entrance and exit rates for class i, respectively. Λ, μ_i and ρ_i are the vital parameters. In the disease free situation the population is assumed to be at demographic equilibrium. γ_i is the recovery rate, m_i the disease induced death rate and β_{ij} is the infection rate between class i and class j. Typically, it will be assumed that $\beta_{ij} = \beta_{ji}$.

The class Q_i has the effect of removing susceptible individuals from the infection dynamics. If $p_i = \lambda_i = 0$ there is no quarantine and the system reduces to an age-structured SEIR model.

TABLE 1. Age Classes.

Class	Age (years)	% Population	% Mortality (year)	μ_i (year)
1	[0,19]	40.2 %	12.6 %	1.959/1000
2	[20,59]	50.5 %	33.2 %	4.109/1000
3	[60,100]	9.3 %	54.2 %	36.425/1000

According to [10] Brazil has 18.67 births and 6.26 deaths by 1000 inhabitants per year, giving an annual population growth of 1.24 %. Let N denote the total population and D the total deaths per year, thus

$$\frac{D}{N} = \mu = \frac{6.25}{1000}\,.$$

Similarly, let D_i and N_i be the number of deaths per year and N_i be the population of age class i respectively. Thus

$$\mu_i = \frac{D_i}{N_i}\,.$$

With this notation the data on Table 1 is denoted by

$$\%\ \text{Population} = \frac{N_i}{N} \text{ and } \%\ \text{Mortality} = \frac{D_i}{D}\,.$$

μ_i is calculated by

$$\mu_i = \frac{D_i}{N_i} = \frac{D_i}{D}\frac{D}{N}\frac{N}{N_i} = \mu\frac{D_i}{D}\frac{N}{N_i} = \mu\frac{(D_i/D)}{(N_i/N)}\,.$$

The disease free steady state is denoted by

$$S_1^*, S_2^*, S_3^*, E_i = I_i = R_i = 0 \quad i = 1, 2, 3, \tag{2.2}$$

where by S_i^* we denote the number of individuals of age class i (all individuals are susceptible, see Table 1). For the model without quarantine, adding the equations for the disease free state gives

$$(S_1(t) + S_2(t) + S_3(t))'(t) = (\Lambda - \mu_1 S_1(t) - \mu_2 S_2(t) - \mu_3 S_3(t))\,.$$

Assuming that the total population is constant and on demographic equilibrium, using the values for the population distribution as the equilibrium values, one must have

$$\Lambda = \mu_1 S_1^* + \mu_2 S_2^* + \mu_3 S_3^* = \frac{6.25}{1000} \text{ deaths/year.}$$

The actual annual growth rate will be ignored. Since the time frame of interest is small compared to the demographic time scale, this has no consequences on the main conclusions of this work. The demographic equilibrium implies that ρ_1 and ρ_2 satisfy

$$\rho_2 = \frac{\mu_3 S_3^*}{S_2^*} = 6.707 \times 10^{-3} \quad \text{and} \quad \rho_1 = \frac{(\mu_2 + \rho_2) S_2^*}{S_1^*} = 11.033 \times 10^{-3}\,.$$

If it is assumed that the demographic, disease and quarantine parameters are equal for all age classes, the above system reduces to the classical SEIR system

TABLE 2. Parameters of the basic SEIR model with vital dynamics.

Parameter	Description
p_i	quarantine entrance rate for class i.
λ_i	quarantine exit rate for class i.
Λ	recruitment rate.
μ_i	natural death rate for class i.
ρ_i	survival rate for class i to class $i+1$ $i \leq 2$.
β_{ij}	pathogen's transmission rate between classes i and j.
σ_i	rate at which exposed of class i convert into the infected class.
γ_i	class i host's recovery rate.
m_i	host's pathogen-induced death rate at class i.

with the quarantine term as suggested by [11]. This will be important for what follows. The parameters for the classical SEIR model will be estimated so that the number of cases predicted by the model compares well with the data. This set of parameters will be used later to adjust the age-structured model 2.1.

3. Unstructured SEIR model

The SEIR model without vital dynamics and with quarantine terms is given by

$$\begin{aligned} Q'(t) &= pS(t) - \lambda Q(t)\,, \\ S'(t) &= -\beta S(t)I(t) - pS(t) + \lambda Q(t)\,, \\ E'(t) &= \beta S(t)\, I(t) - \sigma\, E(t)\,, \\ I'(t) &= \sigma\, E(t) - \gamma I(t)\ , \\ R'(t) &= \gamma I(t)\,. \end{aligned} \tag{3.1}$$

Ignoring the quarantine class ($p = \lambda = 0$) the parameters β, σ and γ can be adjusted so that the SEIR curve fits the data. To achieve that, the difference between the SEIR infected curve and the data curve for the number of infected is minimized (see [12] for algorithm description). The parameters found were

$$\beta^* = 0.8481, \quad \sigma^* = 0.2682, \quad \gamma^* = 0.0870\,. \tag{3.2}$$

The initial conditions used for the algorithm were $\beta = 2.2/2.9$, $\sigma = 1/5.2$ and $\gamma = 1/2.9$. The figure 1 shows the data and the SEIR infected curve using the parameters from (3.2). The considered time interval was 20 days.

Remark 3.1. The model must be considered with care. The curve $I(t)$, as given by the SEIR model, predicts the total number of infected individuals (symptomatic and asymptomatic) at time t. However, to estimate the number of individuals that will need medical care, one needs to know the proportion between the reported and unreported cases. Estimates for the number of unreported cases can be found at [14] and the severity of the reported cases can be found at [3]. Asymptomatic cases can be as high as 75% [7] of all cases; also, ratio estimates of reported to unreported cases goes from 1/1 to 1/20 [14]. These uncertainties must be taken into consideration when using the model to make numerical previsions. The emphasis of this paper is placed on understanding qualitatively efficient ways of controlling the epidemic.

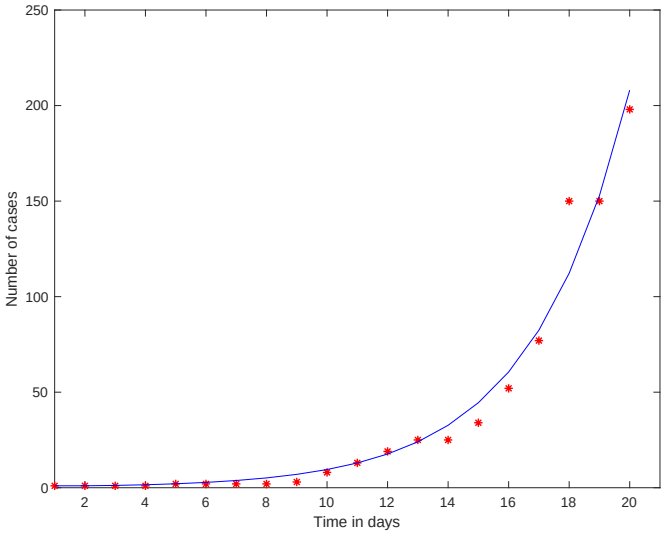

FIGURE 1. The number of infected for the SEIR non-structured model. The parameters values are as in 3.2.

Quarantines will be characterized by two values: the entrance rate p and the exit rate λ. p is composed of two terms, γ_q and ξ. γ_q is the average time it takes for a person to enter quarantine (see [11]) and ξ is a dimensionless multiplicative factor representing the percentage of individuals that in fact voluntarily quarantine. With this notation

$$p = \frac{\xi}{\gamma_q}\,.$$

As an example, suppose that 70% of the population quarantine in an interval of 2 days. Then $p = 0.70/2 = 0.35$. It will be assumed that $p \in [0.0, 0.40]$. $p = 0$ means that there is no quarantine. As in [11] it will be assumed that the time to leave quarantine will between 30 and 60 days, giving that $\lambda \in [1/60, 1/30]$.

Remark 3.2. For future reference we observe that, from definition, p is smaller than the percentage of quarantined population.

The effect of the quarantine on the prevalence curve is twofold: it decreases the maximum $I(t)$ value and postpones the date of its occurrence. To assess the efficiency of the quarantine, the maximum of the prevalence curve and the time of its occurrence were calculated and are shown in Figure 3 .

The important feature on Figure 3 is the existence of a threshold value for the epidemic effort. For values greater than this critical value, the maximum number of infected decreases extremely fast and the maximum time essentially stabilizes. This is a common feature for all p and λ as shown in figure 5.

Critical values for quarantine efforts are clearly seen for the contour plots for the maximum number of infected. The white region on Figure 6 divides the parameter plane in two regions. The region above has a maximum number of infected smaller than 1×10^6 infected (by the above rough estimates ≈ 5000 deaths). The region

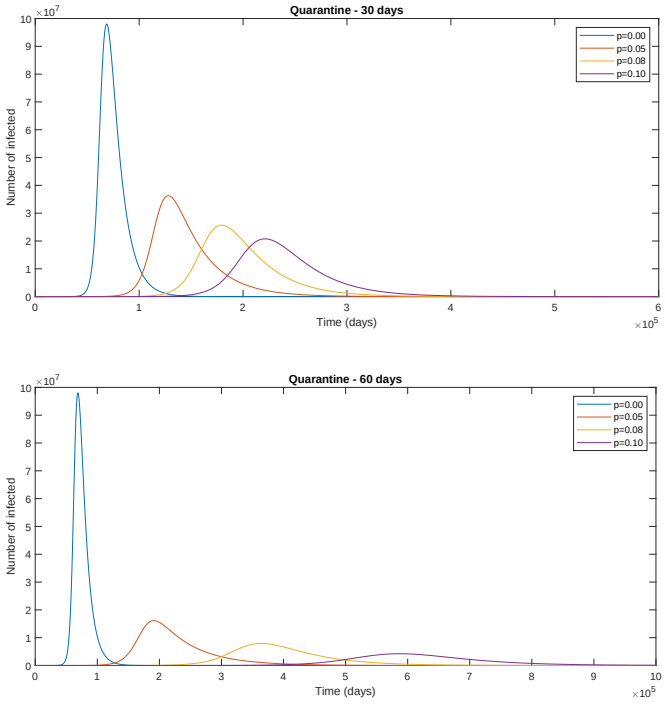

FIGURE 2. Prevalence curve for different quarantine efforts. The top figure assumes a 30 days quarantine and the bottom figure a 45 days quarantine.

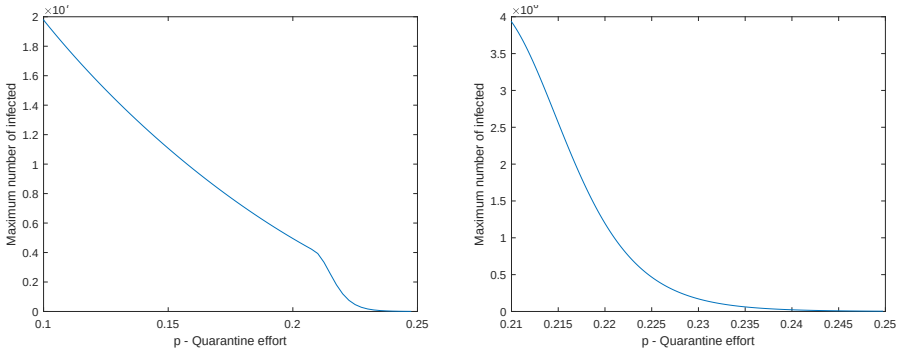

FIGURE 3. Maximum of infected as a function of the quarantine effort p. The figure on the right-hand side details the fast decrease after $p = 0.21$. Quarantine time is 30 days.

below has larger numbers of infected (and of deaths). The level sets accumulate around a critical level set, showing again that, qualitatively, quarantines do work.

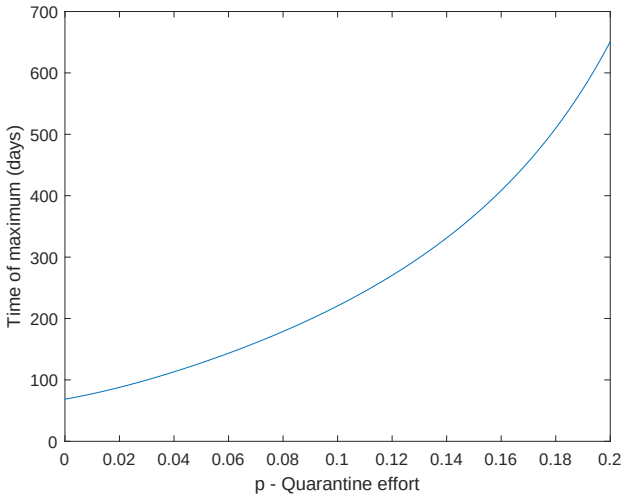

FIGURE 4. The time for the maximum of the epidemic curve as a function of the quarantine effort p. Quarantine time is 30 days.

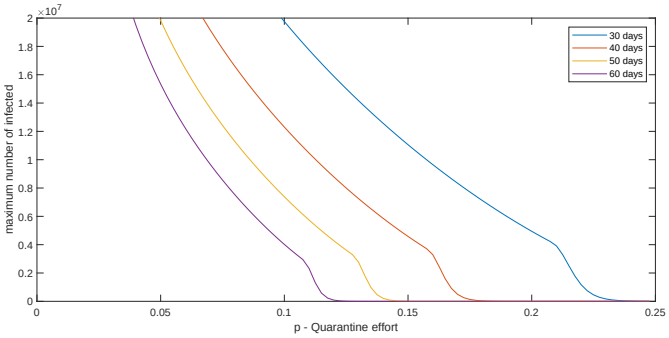

FIGURE 5. The maximum of the epidemic curve as a function of the quarantine effort p for different quarantine values.

4. Control strategies for the age-structured model

The control measures for the age-structured model will be divided in two types. The first type controls the epidemic parameters [2]. This will be made through an R_0 sensitivity analysis: the R_0 for the age-structured model will be numerically determined and its parameter dependence will be investigated. The second type of control will be the age-oriented quarantines. The parameters p_i determine the quarantine effort for each class. Due to the different classes weights on the population composition, and to the different epidemic parameters of each class, this study allows us to assess the impact of each class quarantine on the epidemic dynamics. Before we proceed, we need to adjust the parameters for the structured model.

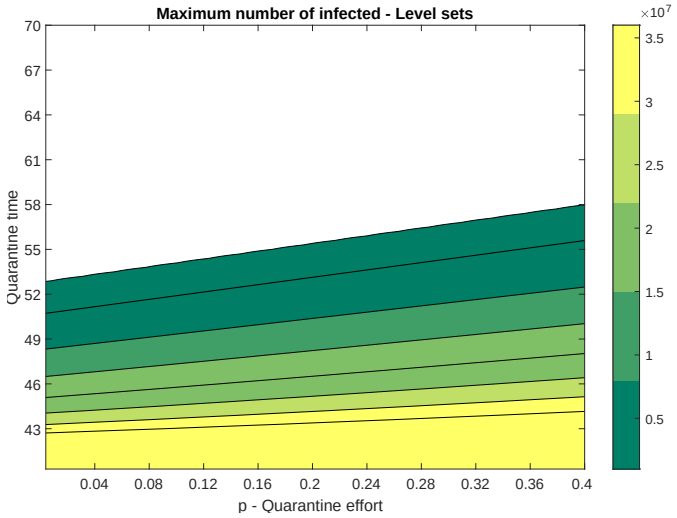

FIGURE 6. Level curves for the maximum number of infected as a function of quarantine effort and quarantine time.

4.1. **Data Fitting.** There are 12 parameters to be determined for the structured model: σ_i, γ_i, $\beta_{ij} = \beta_{ji}$ for $i, j = 1, 2, 3$. The algorithm fits the parameters to the available data of Brazil's total number of reported cases for the first 19 days of infection by a least squares method. The distance between the predicted curve

$$I(t) = I_1(t) + I_2(t) + I_3(t)$$

and the data curve is minimized. The initial parameters for the minimization search algorithm are based on the ones found for the unstructured SEIR model (3) taking into consideration the population percentage of each age class. Let c_i be the population percentage of each class, that is (see Table 1), $c_1 = 0.402$, $c_2 = 0.505$ and $c_3 = 0.093$. The initial values for the iteration are chosen as

$$\sigma_i = c_i \frac{\sigma_i^*}{3}, \quad \gamma_i = c_i \frac{\gamma_i^*}{3} \quad \text{for } i = 1, 2, 3.$$
$$\beta_{ij} = \beta^* \quad \text{for } i \le j = 1, 2, 3\,,$$

The resulting values are listed in Table 3 and a plot of the daily number of infections and the number of reported cases is shown in Figure 7.

4.2. R_0 **Analysis.** In this section R_0 is calculated. To determine the relative importance of model parameters to disease transmission and prevalence we study the effects of these parameters on R_0 through a deterministic sensitivity analysis (refer to [5] for details). R_0 is determined via the next generation approach [8]. It

TABLE 3. Fitted parameters for the age-structured SEIR model without vital dynamics.

Parameter	Value	Parameter	Value
β_{11}	1.76168	σ_1	0.27300
β_{12}	0.36475	σ_2	0.58232
β_{13}	1.32468	σ_3	0.69339
β_{22}	0.63802	γ_1	0.06862
β_{23}	0.35958	γ_2	0.03317
β_{33}	0.57347	γ_3	0.35577

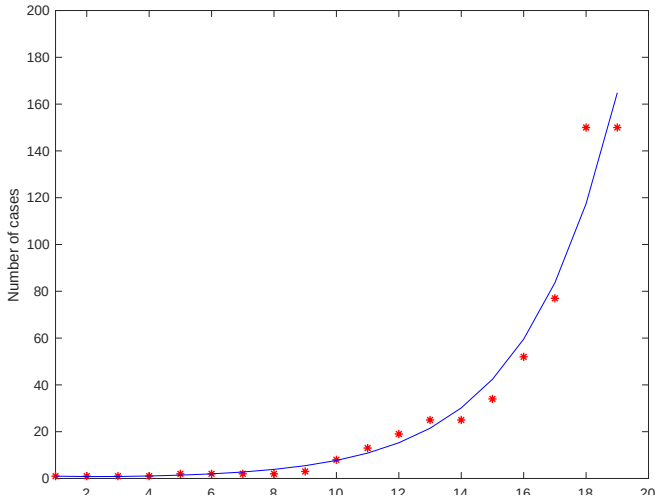

FIGURE 7. The number of infected for the SEIR structured model. Parameter values as in Table 3

equals the spectral radius of FV^{-1}, where

$$F = \begin{pmatrix} 0 & 0 & 0 & \beta_{11}S_1^* & \beta_{12}S_1^* & \beta_{31}S_1^* \\ 0 & 0 & 0 & \beta_{21}S_2^* & \beta_{22}S_2^* & \beta_{23}S_2^* \\ 0 & 0 & 0 & \beta_{31}S_3^* & \beta_{32}S_3^* & \beta_{33}S_3^* \\ 0 & 0 & 0 & 0 & 0 & 0 \\ 0 & 0 & 0 & 0 & 0 & 0 \\ 0 & 0 & 0 & 0 & 0 & 0 \end{pmatrix}$$

and

$$V = \begin{pmatrix} D_1 & 0 & 0 & 0 & 0 & 0 \\ 0 & D_2 & 0 & 0 & 0 & 0 \\ 0 & 0 & D_3 & 0 & 0 & 0 \\ -\sigma_1 & 0 & 0 & \tilde{D}_1 & 0 & 0 \\ 0 & -\sigma_2 & 0 & 0 & \tilde{D}_2 & 0 \\ 0 & 0 & -\sigma_3 & 0 & 0 & \tilde{D}_3 \end{pmatrix},$$

where $D_i = \sigma_i + \mu_i$ and $\tilde{D}_i = \gamma_i + \mu_i + m_i$ for $i \in \{1, 2, 3\}$. Thus

$$FV^{-1} = \begin{pmatrix} K_{11} & K_{12} \\ K_{21} & K_{31} \end{pmatrix},$$

where the block K_{11} is

$$\begin{pmatrix} \frac{\beta_{11}\sigma_1 S_1^*}{\gamma_1(\sigma_1+\mu_1)(\gamma_1+\mu_1+m_1)} & \frac{\beta_{12}\sigma_2 S_1^*}{\gamma_2(\sigma_2+\mu_2)(\gamma_2+\mu_2+m_2)} & \frac{\beta_{13}\sigma_3 S_1^*}{\gamma_3(\sigma_3+\mu_3)(\gamma_3+\mu_3+m_3)} \\ \frac{\beta_{21}\sigma_1 S_2^*}{\gamma_1(\sigma_1+\mu_1)(\gamma_1+\mu_1+m_1)} & \frac{\beta_{22}\sigma_2 S_2^*}{\gamma_2(\sigma_2+\mu_2)(\gamma_2+\mu_2+m_2)} & \frac{\beta_{23}\sigma_3 S_2^*}{\gamma_3(\sigma_3+\mu_3)(\gamma_3+\mu_3+m_3)} \\ \frac{\beta_{31}\sigma_1 S_3^*}{\gamma_1(\sigma_1+\mu_1)(\gamma_1+\mu_1+m_1)} & \frac{\beta_{32}\sigma_2 S_3^*}{\gamma_2(\sigma_2+\mu_2)(\gamma_2+\mu_2+m_2)} & \frac{\beta_{33}\sigma_3 S_3^*}{\gamma_3(\sigma_3+\mu_3)(\gamma_3+\mu_3+m_3)} \end{pmatrix},$$

the block K_{12} is

$$\begin{pmatrix} \frac{\beta_{11}S_1^*}{\gamma_1+\mu_1+m_1} & \frac{\beta_{12}S_1^*}{\gamma_2+\mu_2+m_2} & \frac{\beta_{13}S_1^*}{\gamma_3+\mu_3+m_3} \\ \frac{\beta_{21}S_2^*}{\gamma_1+\mu_1+m_1} & \frac{\beta_{22}S_2^*}{\gamma_2+\mu_2+m_2} & \frac{\beta_{23}S_2^*}{\gamma_3+\mu_3+m_3} \\ \frac{\beta_{31}S_3^*}{\gamma_1+\mu_1+m_1} & \frac{\beta_{32}S_3^*}{\gamma_2+\mu_2+m_2} & \frac{\beta_{33}S_3^*}{\gamma_3+\mu_3+m_3} \end{pmatrix}$$

and K_{21} and K_{22} are the 3×3 zero matrix. Due to the block structure of FV^{-1}, its eigenvalues are easily calculated. However, due to the high number of parameters, their expression is too cumbersome to be of any analytical use. The sensitivity analysis is therefore computed numerically. Figures 8, 9, 10 and 11 show the R_0 parameter dependence.

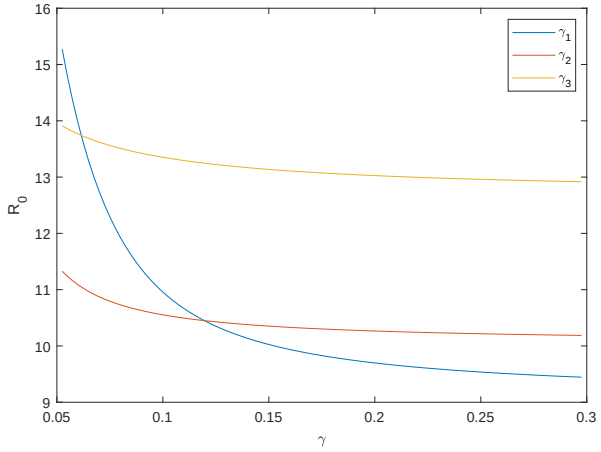

FIGURE 8. R_0 as a γ_i function. Different curves show which γ_i is varying while the others are kept constant.

The use of the parameters of the classical SIR model as control variables was studied in [1]. We will follow its interpretation. Measures as keeping social distance, wearing protective masks, washing hands, etc have the effect of reducing the contact rates β_{ij}. Identifying infected through tests, body temperature checks, etc and putting them into quarantine has the effect of increasing the removal rates γ_i. σ_i is a parameter that can not be controlled.

The results can be summarized as follows:

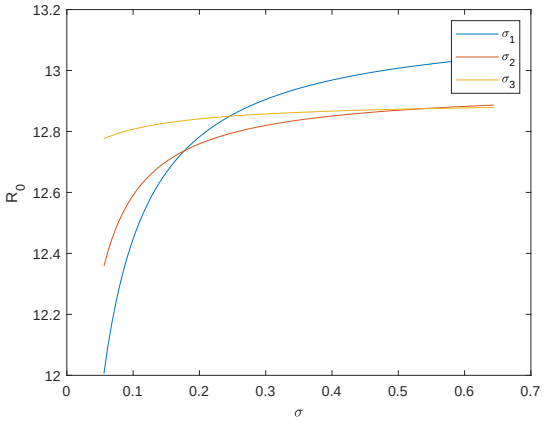

FIGURE 9. R_0 as a σ_i function. Different curves show which σ_i is varying while the others are kept constant.

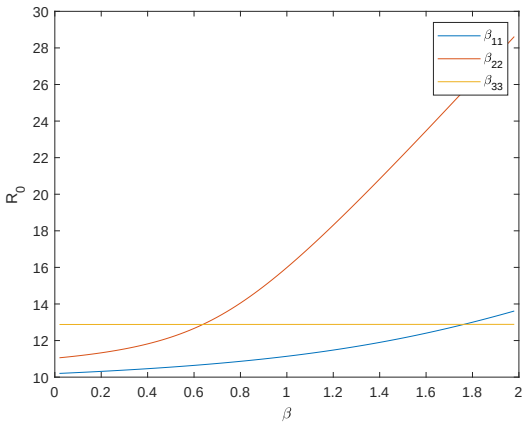

FIGURE 10. R_0 as a β_{ii} function. Different curves show which β_{ii} is varying while the others are kept constant.

(i) Class 1 is the most sensitive to screening measures (see Figure 8). Youngsters should be preferentially screened.
(ii) Considering the direct contacts within the same class, class 2 is the more sensitive (see Figure 10). Social distance between adults has the biggest impact on R_0.
(iii) For the direct contact between different class, β_{12} has the greatest impact on R_0.

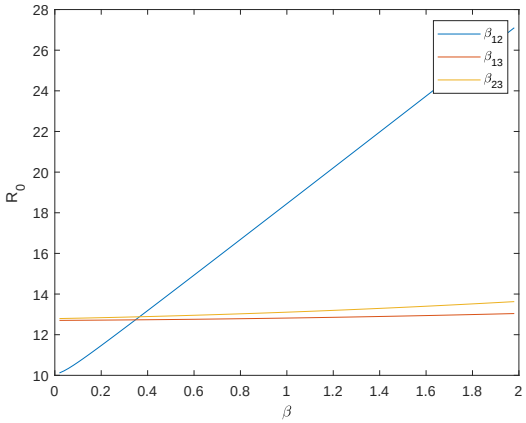

FIGURE 11. R_0 as a β_{ij}, $i < j$ function. Different curves show which β_{ij} is varying while the others are kept constant.

5. Effects of different quarantine policies

In this section we study the impacts of different quarantine strategies. The disease induced mortality rate was taken into account by considering the number of deaths as a fraction of the recovered class. Death rates for all age groups are estimated using the data from [3] (Table 4). As mentioned in Section 3, I_1, I_2 and I_3 include symptomatic and asymptomatic infected individuals as well as unreported cases, so death rates will be multiplied by a factor of 0.25 (since only 25% of the infected are symptomatic [7]) and by 1/20 (due to unreported cases [14]). This leaves us with a multiplicative factor of $\phi = 0.25 * (1/20) = 0.0125$ to estimate the number of deaths. Since we will be working with relative proportions, the actual value of ϕ will be of no importance.

TABLE 4. Death rates for the age-structured model (data taken from [3]).

Age group	Number of cases	Deaths	% Death
1	350	1	0.29%
2	9541	36	0.38%
3	9068	768	8.47%

With these values on hand, we can study the impact of a quarantine with parameters λ and p_i, for $i \in \{1, 2, 3\}$. Calling p the quarantine effort for the unstructured model, it is assumed that the total quarantine effort equals the effort for the unstructured model that is

$$p_1 + p_2 + p_3 = p\,.$$

Remark 5.1. As mentioned in 3.2, calling q_i, $i = 1, 2, 3$, the percentage of quarantined on each age class, it follows that

$$p < q_1 + q_2 + q_3 \leq 1\,.$$

Four different choices for the p_i's will be used, as detailed in Table 5. These are choices for the quarantine effort of each age group. Strategy S1 splits the effort equally among the three groups. Strategy S2 emphasizes a stronger isolation of the elderly (twice as much as the other groups). Strategy S3 enforces isolation of the youngsters and adults twice as much as it does for the elderly. Finally, strategy S4 doubles the quarantine effort on the adults in comparison to the others. To assess the efficiency of these different control strategies, for a fixed control effort p, each control strategy will be calculated for different quarantine times $\lambda \in \{1/30, 1/45, 1/60\}$.

TABLE 5. Quarantine strategies.

Strategy	Choices for the p_i
S1	$p_1 = p/3$, $p_2 = p/3$, $p_3 = p/3$
S2	$p_1 = p/6$, $p_2 = p/6$, $p_3 = 2p/3$
S3	$p_1 = 2p/5$, $p_2 = 2p/5$, $p_3 = p/5$
S4	$p_1 = p/6$, $p_2 = 2p/3$, $p_3 = p/6$

The estimation of the number of deaths can be made by multiplying the number of recovered at the end of the epidemic in each of the three age groups by the death rates from Table 4 and by the multiplicative factor ϕ. However, due to parameters uncertainties and lack of estimations for the parameter p, a different approach is taken. We arbitrarily chose one of the values as unit and calculated all the other results proportionally. The results for $p = 0.2$ are available in Table 6. (For reference only, the number of deaths chosen as unit was 2869).

TABLE 6. Proportion of deaths for each age group for different quarantine strategies and durations.

λ	Age group	S1	S2	S3	S4
1/30	1	1	1.02	0.99	1.03
	2	1.61	1.67	1.59	1.47
	3	7.20	6.43	7.46	7.51
	Total	9.81	9.12	10.04	10.01
1/45	1	0.95	0.99	0.93	1.01
	2	1.51	1.60	1.47	1.29
	3	6.77	5.75	7.18	7.26
	Total	9.23	8.34	9.58	9.56
1/60	1	0.90	0.96	0.88	0.98
	2	1.41	1.54	1.36	1.14
	3	6.38	5.21	6.90	7.01
	Total	8.69	7.71	9.14	9.13

One could argue that the optimal control would occur if we put all the quarantine effort in the isolation of the elderly and no isolation at all for youngsters and adults. With our terminology, this means considering a strategy S5 defined by $p_1 = p_2 = 0$ and $p_3 = p$. However, this leads to two main problems: first, due to the small

percentage of the elder class the quarantine effort would be too small (in fact smaller than 0.1) to be of any significance. Second, it would allow for a much higher number of infected individuals (see Figure 12), hence a great increase in the total of hospitalizations, which would collapse the Health System. Therefore, in order to achieve better quarantine results, the total effort needs to include all age-groups, with more emphasis on the elderly since they have a higher fatality rate due to the disease.

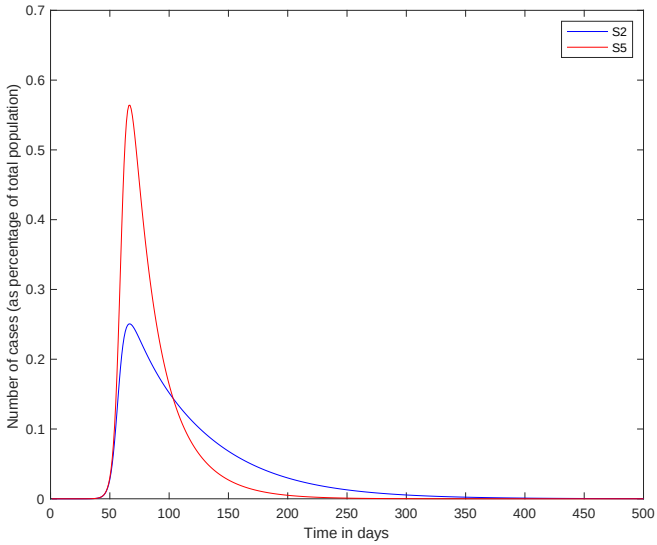

FIGURE 12. Plots of the total number of infected, as percentages of the total population, for strategies S2 and S5. The quarantine parameters were $p = 0.2$ and $\lambda = 1/60$.

Notice that strategy S2 is, by far, the best among these. All other strategies end up with, at least, 7.5% more deaths. We can also analyze the strategies by plotting them. Let μ_i, $i \in \{1, 2, 3\}$, be the death rates from Table 4, so

$$\mathcal{D}_j(t) = \phi \sum_{i=1}^{3} \mu_i R_i(t)$$

converges to the total amount of deaths that result from strategy S_j, $j \in \{1, 2, 3, 4\}$. Figure 13 plots the graphs of $\mathcal{D}_j(t)$, normalized by

$$\lim_{t\to\infty} \mathcal{D}_2(t),$$

produced by the four strategies for different values of p. Notice yet that, in all four cases, the strategy that produces the smallest limit value (hence the smallest death toll) is S2.

6. Conclusions

In this paper we introduced an age-structured SEIR model with a quarantine compartment. Three age classes were used: infants (0 to 19 years), adults (20 to

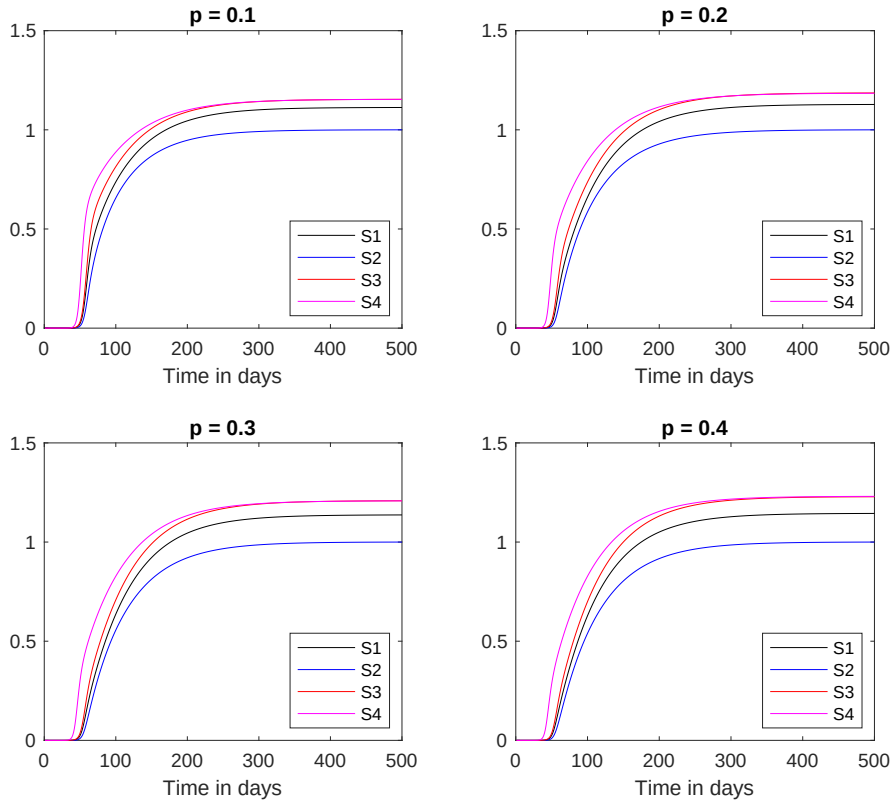

FIGURE 13. Plots of $\mathcal{D}_j(t)$ for $\lambda = \frac{1}{30}$, $j \in \{1, 2, 3, 4\}$.

59 years) and elderly (60 to 100 years). First we studied the associated classical unstructured SEIR model without vital dynamics. The parameters were fitted by a least squares algorithm and the impact of the quarantine parameters p and λ was studied. Our main findings concern the existence of a numerical threshold value for the quarantine parameters: above a certain curve on the (p, λ)-plane, the maximum number of infected decreases in an accentuated way. This shows that an abrupt decline on the number of cases should be observed if the quarantine is being efficient. If this decline is not being observed, quarantine effort and time should be increased.

The parameters obtained for the unstructured SEIR model were used to adjust the parameters for the age-structured SEIR model. Using this data, the basic reproduction number R_0 was calculated and its dependence on the epidemic values was studied. Our findings for the R_0 analysis are as follows:

(i) Class 1 is the most sensitive to screening measures (see Figure 8). Youngsters should be preferentially screened.

(ii) Considering the direct contacts within the same class, class 2 is the more sensitive (see Figure 10). Social distance between adults has the biggest impact on R_0.

(iii) For the direct contact between different class, β_{12} has the greatest impact on R_0.

Finally we studied the impact of age-oriented campaigns considering different strategies and different values of p for the total campaign effort. Recalling that p is bounded by the percentage of quarantined population (see remarks 3.2 and 5.1), our findings show that the highest possible quarantine must be made, and then, this effort must concentrate on putting into quarantine the total of elders and assuring equal proportions of adults and youngsters.

Acknowledgements. The authors would like to thank Renato Mello (IFSP - Campus Salto) for discussions during the preparation of this manuscript.

References

[1] C. Castilho; *Optimal control of an epidemic through educational campaigns.*, Electron. J. Differential Equations, **2006** (2006) no. 125, 1–11.

[2] C. Castillo-Chavez, H.W. Hethcote, V. Andreasen, S.A. Levin, W.M. Liu; *Epidemiological models with age structure, proportionate mixing, and cross-immunity*, Journal of mathematical biology **27** (1989), no. 3, 233–258.

[3] *Centro de coordinación de alertas y emergencias sanitarias goberno españa - enfermedad por el coronavirus (covid-19)*, 2020 (accessed April 4, 2020), https: //www.mscbs.gob.es/profesionales/saludPublica/ccayes/alertasActual/nCov-China/documentos/Actualizacion_52_COVID-19.pdf.

[4] D. Cereda, M. Tirani, F. Rovida, V. Demicheli, M. Ajelli, P. Poletti, F. Trentini, G. Guzzetta, V. Marziano, A. Barone, et al.,; *The early phase of the covid-19 outbreak in lombardy, italy*, arXiv preprint arXiv:2003.09320 (2020).

[5] N. Chitnis, J. M. Hyman, J. M. Cushing; *Determining important parameters in the spread of malaria through the sensitivity analysis of a mathematical model*, Bulletin of mathematical biology **70** (2008), no. 5, 1272.

[6] N. G. Davies, P. Klepac, Y. Liu, K. Prem, M. Jit, R. M. Eggo, CMMID COVID-19 working group, et al.; *Age-dependent effects in the transmission and control of covid-19 epidemics*, MedRxiv (2020).

[7] M. Day; *Covid-19: four fifths of cases are asymptomatic, china figures indicate.*, The BMJ (2020), https: //www.bmj.com/content/369/bmj.m1375.

[8] O. Diekmann, J.A.P. Heesterbeek, J. Metz; *On the definition and the computation of the basic reproduction ratio r_0 in models for infectious diseases in heterogeneous populations*, Journal of mathematical biology, **28** (1990), no. 4, 365–382.

[9] H. Inaba; *Mathematical analysis of an age-structured sir epidemic model with vertical transmission*, Discrete & Continuous Dynamical Systems-B **6** (2006), no. 1, 69.

[10] *Instituto brasileiro de geografia e estatística - sinopse do censo demográfico 2010*, 2011, https: //biblioteca.ibge.gov.br/visualizacao/livros/liv49230.pdf.

[11] J. Jia, J. Ding, S. Liu, G. Liao, J. Li, B. Duan, G. Wang, R. Zhang; *Modeling the control of covid-19: Impact of policy interventions and meteorological factors*, Electron. J. Differential Equations, **2020** (2020 no. 23, 1-24.

[12] M. Martcheva; An Introduction to Mathematical Epidemiology, Springer, 2015.

[13] J. Riou, C. L. Althaus; *Pattern of early human-to-human transmission of wuhan 2019 novel coronavirus (2019-ncov), december 2019 to january 2020*, Eurosurveillance **25** (2020), no. 4, 2000058.

[14] T. Russel; *Using a delay adjusted case fatality ratio to estimate under reporting*, 2020, https: //cmmid.github.io/topics/covid19/severity/global_cfr_estimates.html.

[15] E. Shim, A. Tariq, W. Choi, Y. Lee, G. Chowell; *Transmission potential and severity of covid-19 in south korea*, International Journal of Infectious Diseases (2020).

[16] K. Sun, J. Chen, C. Viboud; *Early epidemiological analysis of the coronavirus disease 2019 outbreak based on crowdsourced data: a population-level observational study*, The Lancet Digital Health (2020).

[17] The Novel Coronavirus Pneumonia Emergency Response Epidemiology Team; *The epidemiological characteristics of an outbreak of 2019 novel coronavirus diseases (covid-19) in china*, China CDC Weekly **41** (2020), no. 2, 145.

[18] H. Thieme; *Disease extinction and disease persistence in age structured epidemic models*, Nonlinear Analysis, Theory, Methods and Applications **47** (2001), no. 9, 6181–6194.

[19] J. T. Wu, K. Leung, G.M. Leung; *Nowcasting and forecasting the potential domestic and international spread of the 2019-ncov outbreak originating in wuhan, china: a modelling study*, The Lancet, **395** (2020), no. 10225, 689–697.

[20] X. Zhao, B. Zhang, P. Li, C. Ma, J. Gu, P. Hou, Z. Guo, H. Wu, Y. Bai; *Incidence, clinical characteristics and prognostic factor of patients with covid-19: a systematic review and meta-analysis*, MedRxiv (2020).

[21] L. Zhou, Y. Wang, Y. Xiao, M.Y. Li; *Global dynamics of a discrete age-structured sir epidemic model with applications to measles vaccination strategies*, Mathematical biosciences **308** (2019), 27–37.

[22] Y. Zhou, P. Fergola; *Dynamics of a discrete age-structured sis models*, Discrete & Continuous Dynamical Systems-B **4** (2004), no. 3, 841.

César Castilho
Departamento de Matemática, Universidade Federal de Pernambuco, Recife, PE CEP 50740-540 Brazil
Email address: castilho@dmat.ufpe.br

João A. M. Gondim
Unidade Acadêmica do Cabo de Santo Agostinho, Universidade Federal Rural de Pernambuco, Cabo de Santo Agostinho, PE CEP 54518-430 Brazil
Email address: joao@dmat.ufpe.br

Marcelo Marchesin
Departamento de Matemática, Universidade Federal de Minas Gerais, Belo Horizonte, MG CEP 31270-000 Brazil
Email address: mdm@mat.ufmg.br

Mehran Sabeti
Instituto de Ciências Exatas e Tecnológicas, Universidade Federal de Viçosa Campus-Florestal, Viçosa, MG CEP 35690-000 Brazil
Email address: mehran@ufv.br